

Article

Measurement of quasi-static and dynamic displacements of footbridges using the composite instrument of smartstation and accelerometer: case studies

Jiayong Yu ^{1,*}, Zhen Fang ¹, Xiaolin Meng ^{1,2}, Yilin Xie ³ and Qian fan ⁴

¹ Key Laboratory for Wind and Bridge Engineering of Hunan Province, Hunan University, Changsha 410082, Hunan, China; surveying@hnu.edu.cn (J.Y.); fangzhen2@hnu.edu.cn (Z.F.);

² Nottingham Geospatial Institute/Sino-UK Geospatial Engineering Centre, The University of Nottingham, Nottingham NG7 2TU, UK; xiaolin.meng@nottingham.ac.uk

³ Jiangsu Hydraulic Research Institute, Nanjing 210017, Jiangsu, China; xieyilin-1983@163.com

⁴ College of Civil Engineering, Fuzhou University, Fuzhou, China; fanqian@fzu.edu.cn

* Correspondence: surveying@hnu.edu.cn

Abstract: Dynamic response monitoring of bridge structures has received considerable attention. It is important to synchronously measure both quasi-static and dynamic displacements of bridge structures. However, traditional accelerometer method cannot capture quasi-static displacement component although it can detect dynamic displacement component. To this end, a novel composite instrument of smartstation was proposed to monitor vibration displacements of footbridges. Full-scale experiments were conducted on a footbridge to validate the feasibility of the composite instrument-based monitoring method. Chebyshev filter and wavelet algorithms were developed to process the composite instrument measurements. Conclusions were drawn that the measurement noise of the composite instrument mainly distributed in a frequency range of 0 - 0.1 Hz. In two case studies with displacement peaks of 5.7 - 10.0 mm and 1.3 to 2.5 mm, the composite instrument accurately identified their quasi-static and dynamic displacements. The composite instrument will be a potential tool for structural dynamic monitoring with the enhancement of its overall performance.

Keywords: composite instrument of smartstation; accelerometer; dynamic displacement; vibration frequency; structural health monitoring

1. Introduction

The measurement of three-dimensional quasi-static and dynamic displacements of bridge structures is an important task for structural health monitoring [1]. Vibration displacements of bridge structures were usually measured by traditional methods such as Global Navigation Satellite System (GNSS) and accelerometer. The GNSS technologies are capable of identifying dynamic displacement components (instantaneous deformation) at a millimeter-level accuracy with a sampling rate up to 20 Hz, even 100 Hz [2, 3]. However, when they are used to identify quasi-static displacement components induced by temperature changes, vehicle loads, their measurement accuracies are limited within a relatively low range from 10 to 20 mm because of signal multipath errors [4, 5]. Moreover, the accelerometer is capable of accurately detecting dynamic displacements of bridges by double integrations of accelerations, but quasi-static displacements of bridges cannot detect at all because of drift errors when the excitation term is relatively longer [6, 7].

In order to solve the above-mentioned problem, a composite instrument of smartstation was proposed to synchronously monitor both dynamic and quasi-static displacements of bridge structures. The composite instrument combines a high performance Robotic Total Station (RTS, also

called Terrestrial Positioning System, TPS), and a powerful GNSS unit in one instrument. The GNSS unit is fully integrated into RTS, rather than a simple combination of two sensors.

The greatest advantage of the composite instrument of the smartstation can accurately capture not only three-dimensional coordinates of the monitored target, but also the GPS (Global Positioning System) time information with a nanosecond-level accuracy. The GPS time information is very important for multi-sensor data fusion. A prototype of smartstation system was designed and developed for the first time by Ingensand et al (1993). The invention concerns a terrestrial surveying system comprising an electro-optic total station for combined measurement of angle and distance, a connection, and a receiver for a satellite position-measuring system [8]. In order to evaluate the composite instrument of the smartstation, a case survey has been conducted on the Porte Palatine, an archaeological building site in Turin. The composite instrument-based technique is considered as a valuable solution for culture heritage survey [9]. The technique was widely employed in many survey scenario such as topography survey, boundary survey, construction site stakeout and utilities survey [10].

The composite instrument was used to monitor dynamic responses of bridge structures in this study. A Leica TCA2003 RTS instrument was used to monitor structural dynamic responses of the Wilford Suspension bridge in Nottingham, UK. However, very little movement of the bridge was measured due to its slow data sampling-rate 1 Hz [11]. Ambient vibration measurements of the Bosphorus Suspension Bridge in Turkey were conducted using a TCA 2003 RTS instrument [12]. Seven vertical and lateral frequencies were detected from the RTS measurements, which lay in the frequency range of 0- 0.5 Hz. A new generation instrument of Leica 1201 RTS with a nominal sampling-rate 10 Hz was used to monitored the dynamic responses of the Gorgopotamos railway bridge in Greece, in response to passing trains [13, 14]. The vertical displacements of the bridge with peaks of 2.5 to 6 mm, and its dominant frequencies distributing in a frequency range of 3.18 – 3.63 Hz were successfully identified [13, 14]. The collocated sensors consisting of RTS, GNSS and accelerometer were adopted to measure displacements of a stiff footbridge in Greece, which were capable of measuring three-dimensional deflections with amplitudes of a few millimeters and identifying oscillation frequencies [15]. To overcome the RTS shortcoming of low data sampling-rate, two approaches were presented to increase RTS sampling-rate from 10 Hz to 20 Hz for determining the vertical displacements of bridges [16]. A conclusion was drawn that the geodetic instruments, GNSS and RTS, in combination with accelerometers can be used to measure with safety semi-static and dynamic deflections of stiff bridges [17]. It is believed that the composite instrument of the smartstation will show better overall performance than the RTS because of its updated hardware and software [10].

The focus of this case study is on the verification of the feasibility of using the composite instrument to monitor bridge dynamic responses. Background noise in three directions in composite instrument measurements were obtained and analyzed in the time-frequency domain for the purpose of characterizing the smartstation measurement noise. The composite instrument was used to monitor dynamic responses of the studied footbridge, induced by a group of three people jumping, and gentle wind and occasional pedestrians, respectively. The quasi-static and dynamic displacements of the footbridge were accurately detected by the composite instrument.

2. Instrumentation and the studied footbridge

2.1 Composite instrument of the smartstation

The composite instrument of the smartstation (Figure 1) was employed in dynamic deformation monitoring of the studied footbridge in this study. The composite instrument combines a high-performance Leica TS30 robotic total station (RTS, also called Terrestrial Positioning System, TPS), and a powerful Leica ATX1230+ GNSS smart-antenna in one instrument. The GNSS unit is fully integrated into RTS. All data are stored in the same database on the same CompactFlash card; all GNSS and RTS operations are controlled via the RTK keyboard with the entire software in the RTS; all measurement, status and other information are displayed on the RTS screen (Figure 1).

The composite instrument with the capability of Automatic Target Recognition (ATR) allows dynamic tracking of targets quickly in three dimensions. The composite instrument can continuously obtain not only three-dimensional coordinates of a prism with a true sample-rate of up to 5-7 Hz, but also the nanosecond-level GPS time information in each record. The composite instrument is one of the best performance coordinate measurement instruments, with an angle measurement accuracy of $\pm 0.5''$ and a distance measurement accuracy of 0.6 mm + 1 ppm.

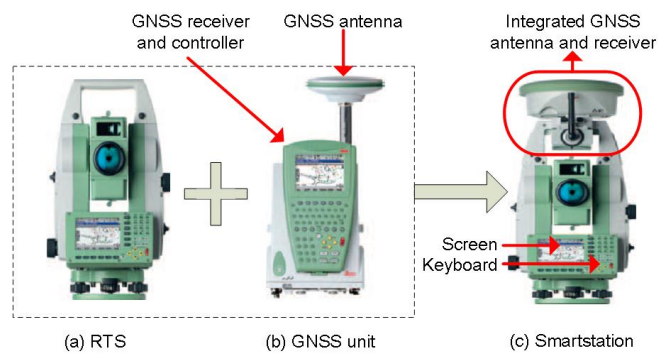


Figure 1. The composite instrument of the smartstation. The composite instrument combines a high-performance Leica TS30 Robotic Total Station -RTS (a) and a powerful Leica GNSS unit (b) in one instrument.

2.2 Accelerometer and Precise Time Data Logger

A Kistler 8392A2 triaxial accelerometer with a data sample-rate of 150 Hz was used to monitor the bridge dynamic responses to verify the composite instrument results. For the purpose of solving the problem of time synchronization, A Precise Time Data Logger (PTDL) was applied to record accelerator data (Figure 2c). It can tag GPS time onto the external data from the accelerometer because it contains a built-in low-cost GPS chip and a small antenna [18]. Thus, the data from both the composite instrument and the accelerator can be applied for data fusion or comparison based on the same GPS time system.

2.3 The description of the Nottingham Wilford Suspension Bridge

Full-scale experiments were performed on the Wilford Suspension Bridge in Nottingham, UK (Figure 2a). The bridge, also known as Meadows Suspension Bridge, is a combined suspension pedestrian footbridge and aqueduct which crossed the River Trent, linking the town of West Bridgford to the Meadows. The historical bridge was constructed in 1904 with a 69.0-m-length main span. Following a restoration in 1983, it was closed to pedestrians in 2008 for a major restoration because of the falling debris from the bridge deck. In the last two decades, the bridge was utilized as the testbed for the purpose of the monitoring researches with innovative sensors and approaches. The first three modal frequencies of the stiff bridge, i.e. 1.44 Hz, 2.79 Hz and 4.66 Hz, have been computed with its finite element model in previous research [19]. The modal parameters of the bridge might change due to the major restoration in 2008.

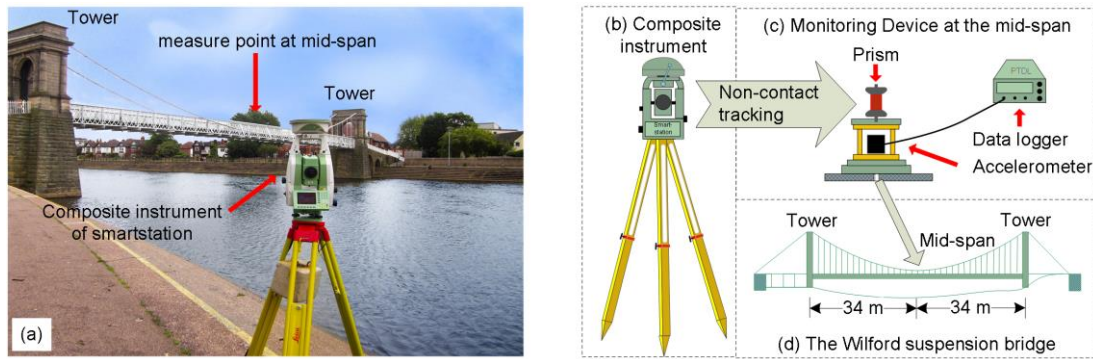


Figure 2. The Wilford suspension bridge in Nottingham and instrumentation. A composite instrument of smartstation was set near the bridge for structural dynamic response monitoring (a); the composite instrument (b) in non-contact mode locked and tracked a 360° prism that was installed upside a cage with a triaxial accelerometer, connected to a Precise Time Data Logger (c); the monitoring devices were fixed at the mid-span of the footbridge for dynamic response monitoring (d).

Table 1. The details of three experimental cases.

Case	GPS time	Description	Instrumentation
1	From second 314100 to 314700, GPS week 1768	Measuring background noise in measurements of the composite instrument	A composite instrument of smartstation
2	From second 312500 to 313700, GPS week 1698	Measuring three people jumping - induced vibrations of the footbridge	A composite instrument and a tri-axial accelerometer
3	From second 476100 to 477300, GPS week 1699	Measuring gentle wind and occasional pedestrian-induced vibrations of the footbridge	A composite instrument and a tri-axial accelerometer

3. Methodology of field measurements

Three experiments with different working conditions were performed in this study (Table 1). Before full-scale experiments, a static experiment (Case 1) was carried out on the campus of the University of Nottingham to understand noise characteristics in measurements of the composite instrument. The other two full-scale experiments were conducted on the Wilford suspension bridge in Nottingham to verify the measurement of vibration displacements of footbridges using the composite instrument. In cases of 2 and 3, vibration displacements of the footbridge were monitored by the composite instrument, which were induced by three people jumping, and gentle wind and occasional pedestrian (Case 3), respectively. The Vibration displacements covers both quasi-static and dynamic displacement components.

In the static experiment of case 1, the composite instrument and the prism were mounted on two tripods, respectively. Two tripods were setup on two stable sites on the campus of the University of Nottingham, with a distance 60 m between these two tripods. The 3D coordinates of the prism were measured and recorded continuously by the composite instrument with a true sample-rate of 5~7 Hz. A three-axis coordinate system is constructed with the x-axis aligned with the measure direction from the composite instrument to the prim, and the z-axis coincident with the gravity direction. Because the prism is not moving, any displacements found in the composite instrument observations can be regarded as background noise [20, 21]. We acquired the background noise in three directions covering

about 60 min. We emphatically analyzed a 600-second-long displacement time series from 314100 second to 314700 second, GPS week 1768.

In the full-scale experiment of case 2, the instrument station of the composite instrument was set up on stable site A2, located at the downstream side of the footbridge, 67.2 m away from the measure point the mid-span of the footbridge (Figure 3). The composite instrument acquired vibration displacements of the measure point with a true sample-rate of 5~7 Hz. The backsight point of the composite instrument was set at the upstream (north) side of the studied bridge, approximately 74.8 m away from the corresponding instrument station. It is necessary to choose a right site as the backsight point because of the need of the intervisibility between the backsight point and the instrument station. The measure point was set at the midspan of the footbridge. Monitoring devices were installed at the measure point of the midspan, covering a Leica GRZ122 360° prism, a Kistler 8392A2 triaxial accelerometer, PTDL Data Logger produced by the research team of the University of Nottingham, and a special cage. The special cage was fixed on the rail of the midspan of the footbridge. The accelerometer was fixed inside the cage whereas the prism was installed upside the cage (Figure 2c). The PTDL data logger was adopted to record accelerometer data in GPS time system, with a data sampling-rate 100 Hz.

The forced vibrations of the footbridge were monitored by both the composite instrument and accelerometer sensors in case 2, which were induced by three people jumping synchronously at its midspan with an interval of several minutes. We acquired synchronously both displacement and acceleration time series from 312500 second to 313700 second, GPS week 1698.

In the full-scale experiment of case 3, the instrument station location was set at the site A3, 64.4 m away from the measure point of the footbridge (Figure 3). Similar to the previous case, the vibration responses of the footbridge were measured by both the composite instrument and accelerometer sensors, which were induced mainly by gentle wind and occasional pedestrians. We acquired synchronously one set of 1200-second-long displacement time series and one set of 1200-second-long acceleration time series from 476100 second to 477300 second, GPS week 1699.

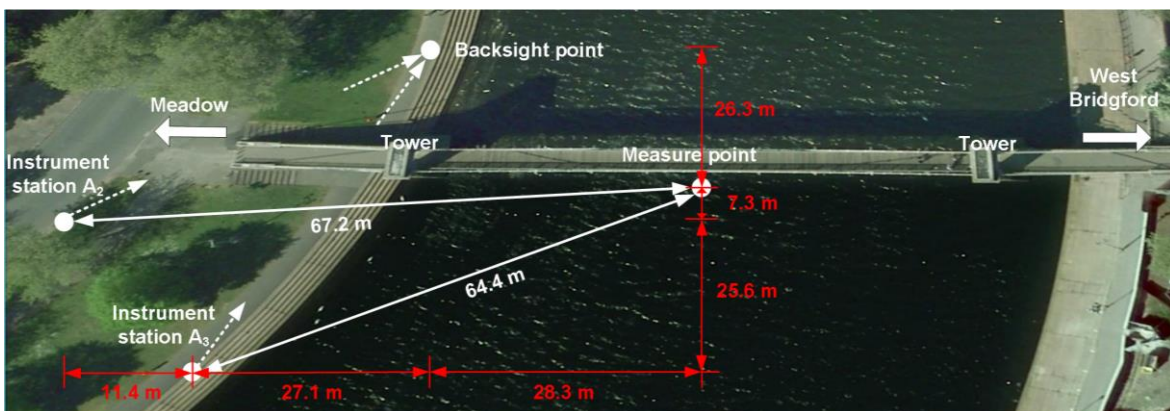


Figure 3. Instrument layout of full-scale experiments performed on the Wilford suspension bridge.

The instrument stations of the composite instrument were set at the sites of A2 and A3 in cases 2 and 3, respectively; The backsight point was set at the upstream (north) side of the bridge; the measure point was set at the mid-span of the studied footbridge.

4. Results and discussion

The background noise in measurements of the composite instrument were detailed in the time-domain frequency by the Continuous Morlet Wavelet Transform (CMWT) algorithm. The dynamic responses of the studied footbridge in two cases were monitored and identified by the composite instrument, which were induced by a group of three people jumping, and gentle wind and occasional pedestrian.

4.1 Background noise in the composite-instrument measurements

In order to characterize measurement noise of the composite instrument in detail, a set of displacement time series in three directions were acquired by the composite instrument in the static experiment of case 1). The displacements in each record include point number, GPS time, x-coordinate, y-coordinate and z-coordinate. A standardized identification procedure was used to preliminarily processed these original records for the purpose of removing duplicates and outliers, recovering missing-records, and so on [21]. Firstly, the duplicate records with identical recording time were removed from the original records, which were caused by the high data-recording rate of the composite instrument. Secondly, the outliers were removed from the original displacement records by a threshold of triple standard deviation. Finally, the missing records were recovered by a linear interpolation method according to the time interval of 0.1 s between two adjacent records. The MATLAB codes were developed to preliminarily process those original records with the above methods by authors.

Figure 4 graphically depicts the profile of the background noise in the measurements of the composite instrument in three directions when the composite instrument is 60 m away from the prism. The amplitudes of background noise fluctuate between 0.6 mm and -1.4 mm in x-axis, between 1.0 mm and -0.9 mm in y-axis, and between 0.8 mm and -1.1 mm in z-axis (vertical direction). In horizontal plane, x-axis is coincident with the sighting line of the composite instrument whereas y-axis is perpendicular to the sighting line. All of Standard Deviations (SD) and Mean Absolute Errors (MAE) of the background noise in each direction are no more than ± 0.5 mm (Table 2). The result shows that the measurement accuracies of the composite instrument monitoring technique can meet the requirements of dynamic deformation monitoring of footbridges.

Figure 5 graphically depicts the time-frequency domain characteristics of the composite instrument measurement noise, corresponding to the displacements shown in Figure 4. The spectra of background noise in three directions were produced using the CMWT algorithm [22, 23].

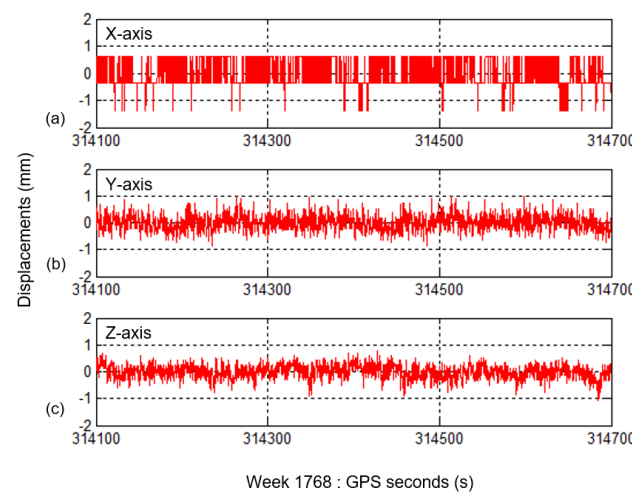


Figure 4. Time histories of background noise in the composite instrument measurements in experimental case 1. The prism was set up on a stable site, 60 m away from the composite instrument.

Table 2. Standard deviations (SD) and mean absolute errors (MAE) of background noise in the composite instrument measurements.

Direction	SD (mm)	MAE (mm)
x-axis	± 0.5	0.4
y- axis	± 0.3	0.2
z- axis	± 0.2	0.2

It is noted that the noise mainly distributes in a frequency range of no more than 0.1 Hz, which are caused by the angle and distance measurement errors of the composite instrument. The noise energy in a frequency range of more than 0.1 Hz is relatively low, which are mainly caused by instrument self-noise such as gaussian noise, white noise [24]. Besides, it is obvious that the noise energy in z-axis is lower than ones in x- and y-axes. The characteristic agrees well with the SD and MAE values of the background noise in the composite instrument measurements as shown in Table 2. The accuracies of horizontal displacements are determined by the horizontal-angle and distance measurements; the accuracies of vertical displacements are determined by the vertical-angle and distance measurements. Horizontal angle accuracies are usually lower than vertical angle accuracies because horizontal angle measurements need a horizontal orientation angle. The previous reasons result in the displacement measurement accuracies in z-axis direction (vertical direction) are relatively higher than those in other directions.

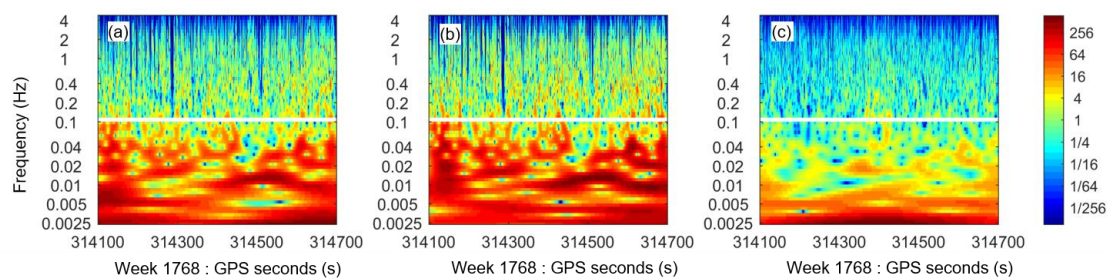


Figure 5. The CMWT-based spectra of the measurement noise of the composite instrument in the x-axis (a), y-axis (b) and z-axis (c), corresponding to displacement time series in Figure 4, with white lines indicating the frequency 0.1 Hz.

4.2 Three people jumping-induced vibrations

In experimental case 2, both the composite instrument and accelerometer sensors were used to monitor dynamic responses of the Wilford Suspension Bridge, which were excited by a group of three people synchronously jumping around 10 s each time on its midspan. A set of 1200 s displacement time series with an interval of 0.1 s were acquired by the composite instrument. Also, a set of 1200 s acceleration time series were synchronously acquired with an interval of 0.01 s by the accelerometer in the same GPS time frame. Using codes written by authors, these two groups of time series have been preliminarily processed to remove duplicates and outliers, and recover missing-records, as the previous case.

Figs. 6a-b. graphically depicts overall vibration displacements of the footbridge in the longitudinal and lateral directions measured by the composite instrument. Although the vibration displacements of the footbridge are very small in both the longitudinal and lateral directions, they are sensitively and accurately measured by the composite instrument. The longitudinal displacements change between 1.0 mm and -1.3 mm with SD of ± 0.3 mm. The lateral displacements change between 1.6 mm and -1.7 mm, with SD of ± 0.5 mm. Figure 6c graphically depicts vibration displacements of the footbridge in vertical direction, measured by the composite instrument. Five significant displacement peaks in vertical direction are correspond to the five times of three-people jumping at the midspan of the footbridge.

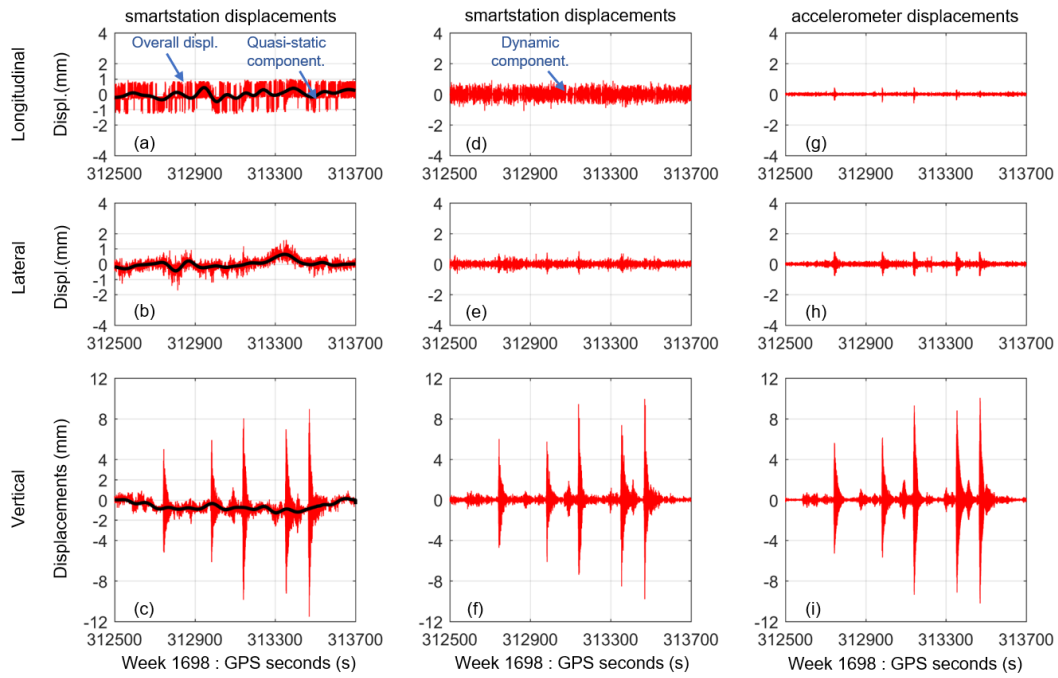


Figure 6. Displacement time series of the footbridge in longitudinal, lateral and vertical directions excited by a group of three people jumping in experimental case 2. The vibration displacements of the footbridge measured by the composite instrument (the red curves in left column) were separated into two parts, i.e., the quasi-static displacements (the black curves in left column) and dynamic displacements (central column). The dynamic displacements are also computed from the accelerometer measurements by double integration (right column).

The smartstaiton-measured vibration displacements of the footbridge were separated into two components, i.e., quasi-static displacements, and dynamic displacements using the Chebyshev high pass filter [25, 26]. Also, the dynamic displacements of the footbridge (seeing right column of Figure 6) were computed from the accelerometer data by double integration [6, 27], which were used for validating the composite instrument results. It is known that quasi-static displacements of the footbridge cannot be derived from the accelerometer data because of the trend errors [28].

Although all quasi-static displacements of the footbridge in three directions have low amplitudes of about 1 mm (seeing the black curves in left column of Figure 6), the composite instrument can accurately detect these quasi-static displacement components. It is to say that measurement errors of the composite instrument should be lower than a millimeter. The curve of the vertical quasi-static displacements shows a strong correlation between vertical deflections and experimenter loads (Fig 6c). When three people walk onto the bridge at first tens of seconds of the experiment, the curve of the vertical quasi-static displacements shows a gradual downward tendency. When three people stay on the midspan of the footbridge, the vertical quasi-static displacements fluctuate close to 1 millimeter. When three people walk out the footbridge at the end of the experiment, the vertical quasi-static displacements recover to zero value.

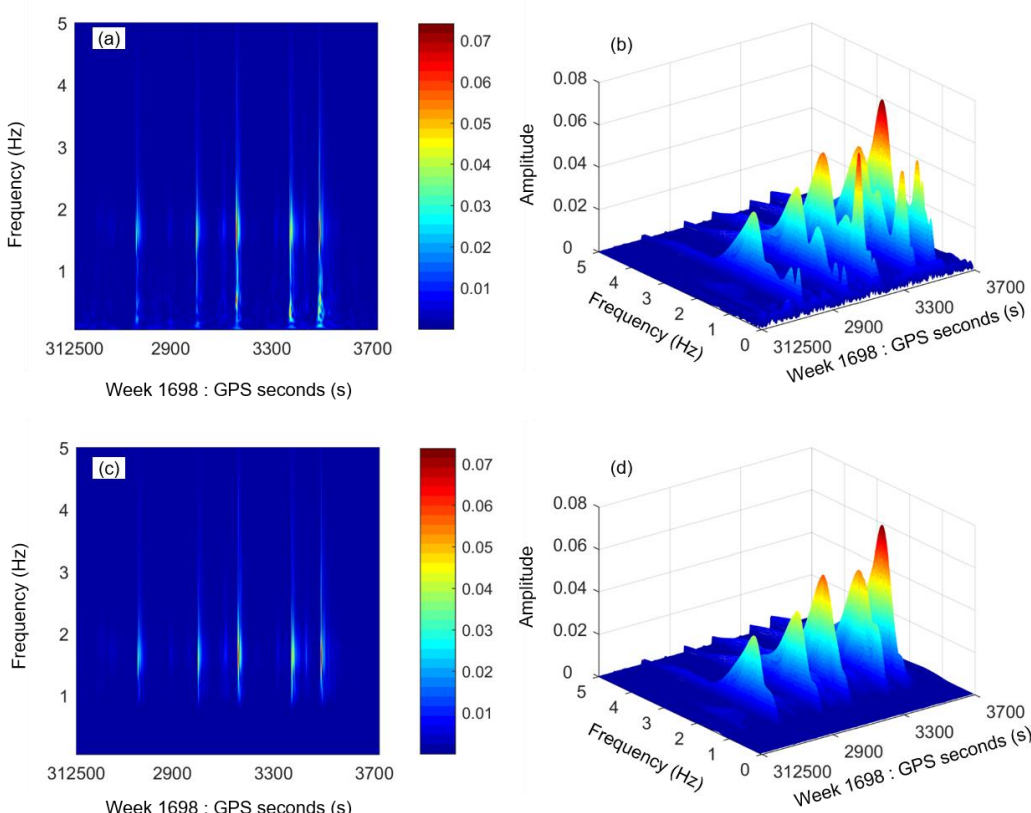
Two sets of dynamic displacements of the footbridge are derived from the composite instrument and accelerometer data, respectively (seeing the center and right columns of Figure 6). It is obvious that they are similar to each other in each direction. In both the longitudinal and lateral directions, the dynamic displacements have small amplitudes of lower than a half-millimeter. It is to say that measurement errors of the composite instrument should be lower than a half-millimeter. The dynamic displacements computed from accelerometer data have relatively lower amplitudes than the ones computed from the composite instrument data. The main reason is that random noise of accelerometer data has been partly eliminated during computing displacements from accelerations.

In vertical direction, both two sets of dynamic displacements as shown in Figs. 6f and 6i depict five significant peaks, corresponding to five sets of three-people jumping, respectively. The corresponding peak differences between these two sets of dynamic displacements are less than 1.0 mm; their peak difference ratios are no more than 10.0% (Table 3). It is shown that the composite instrument can accurately measure dynamic displacements of footbridge with peak values of several millimeters (from 5.7 mm to 10.0 mm).

Table 3. Comparison of peak values of two sets of dynamic displacements in vertical direction derived from the composite instrument and accelerometer measurements in case 2.

Event	Peak displacements / mm		Diff. / mm (①-②)	Ratio / % (①-②)/②
	composite instrument①	Accelerometer②		
1	6.0	5.6	0.4	7.1
2	5.7	6.1	-0.4	6.6
3	9.5	9.3	0.2	2.2
4	7.7	8.6	-0.9	10.0
5	10.0	10.1	-0.1	0.1

Figure 7 graphically depicts three pairs of wavelet-based spectra of overall vibration displacements and dynamic displacements derived from the composite instrument data, and dynamic displacements derived from the accelerometer measurements in vertical direction. These wavelet-based spectra provide local characteristics for the displacement time series. Each three-dimensional spectrum shows five significant displacement peaks, corresponding to five groups of three-people jumping at the midspan of the footbridge. The three-dimensional spectrum of overall vibration displacements shows significant differences with other two three-dimensional spectra of dynamic displacements. The reason is that the overall vibration displacements covers relatively higher random noise and quasi-static displacement components. It is similar to each other between two spectra of dynamic displacements derived from the composite instrument and accelerometer data, respectively.



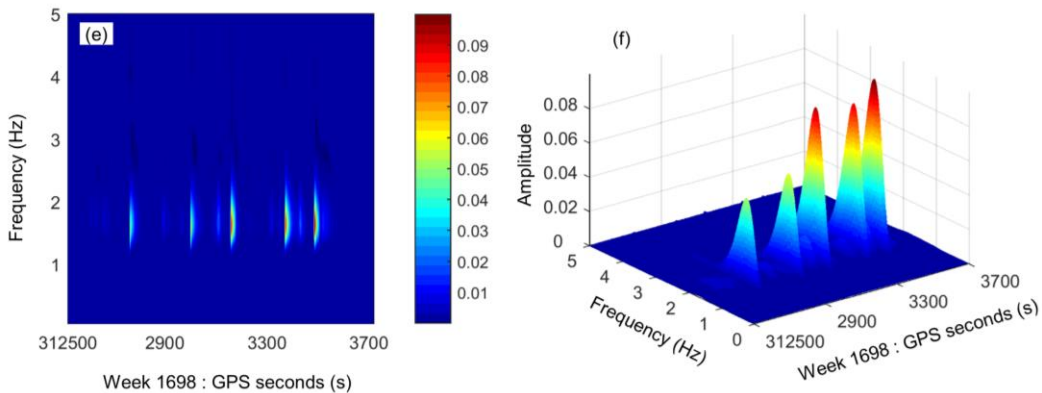


Figure 7. Wavelet-based spectra of displacement time series in vertical direction: two- and three-dimensional spectra of overall vibration displacements (a, b) and dynamic displacements (c, d) derived from the composite instrument data, and dynamic displacements (e, f) derived from the accelerometer data.

4.3 Wind and occasional pedestrian-induced vibrations

Vibration responses of the footbridge, induced by gentle wind and occasional pedestrians, were monitored in experimental case 3. We synchronously acquired 1200-second vibration displacements of the footbridge using the composite instrument, and 1200-second accelerations using the accelerometer in the same GPS time frame. The composite instrument acquired data with a true sampling-rate of 5~7 Hz whereas the accelerometer acquired data with a sample-rate of 100 Hz.

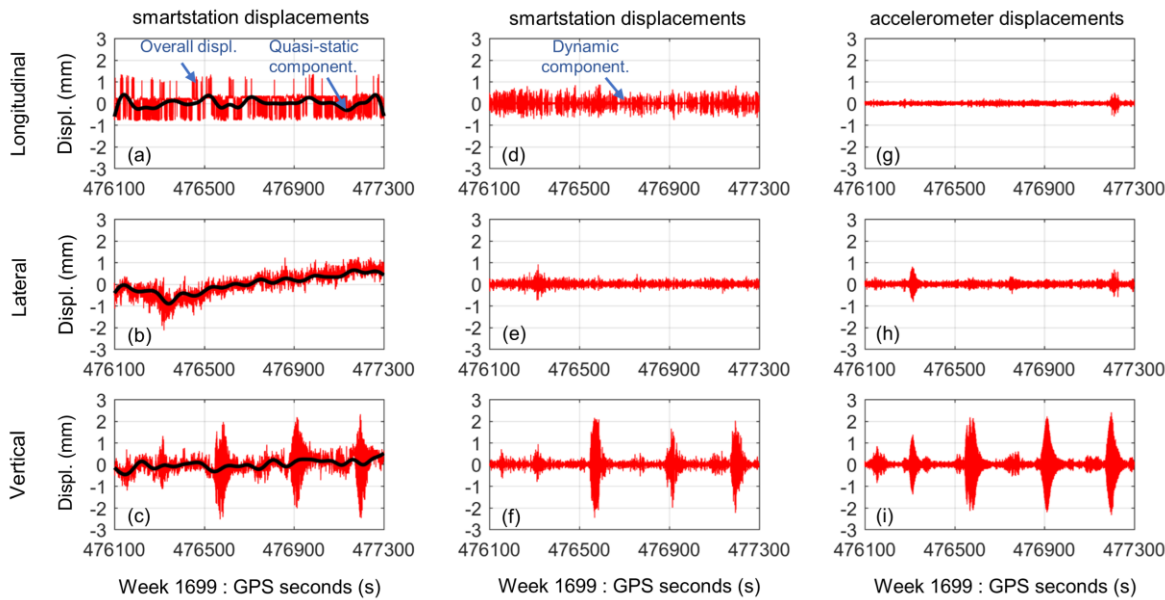


Figure 8. Time histories of displacements of the footbridge in three directions induced by gentle wind and occasional pedestrian in experimental case 3. The overall vibration displacements measured by the composite instrument (the red curves in left column) were separated into two parts, i.e., the quasi-static displacements (the black curves in left column) and dynamic displacements (central column). The dynamic displacements (right column) are also computed from the accelerometer data by double integration.

Figures 8a-c. graphically depicts overall vibration displacements of the footbridge in three directions measured by the composite instrument. They have been preliminarily processed to remove duplicates and outliers, and recover missing-records as previously. All of these displacements in

three directions have small amplitudes with maximal amplitudes of 1.3 mm, 2.1 mm, and 2.5 mm in the longitudinal, lateral and vertical directions, respectively. It is obvious that the composite instrument can sensitively identify the vibration displacements although the vibration displacements only have maximal amplitudes of about 2 mm.

Quasi-static displacements of the footbridge were also identified from the composite instrument data, which were depicted using black curves in the left column of Figure 8. They fluctuate within an amplitude of 1 mm, which caused by the thermal expansion, wind, pedestrian-weight and so on. Two sets of dynamic displacements of the footbridge in three directions were derived from both the composite instrument and accelerometer data, which were depicted as shown in central and right columns of Figure 8, respectively. In each direction, both dynamic displacements derived from the composite instrument and accelerometer data are similar to each other. In vertical direction, three peak values of the dynamic displacements derived from the composite instrument data are about 2 mm, which are agree well with the ones of the dynamic displacements derived from accelerometer data. It is conformed once again that the composite instrument can measure dynamic displacements with maximum amplitudes of about 2 mm.

The modal frequencies of the footbridge in vertical direction were identified using Fast Fourier Transform (FFT) method (Figure 9). The modal frequencies of 1.677 Hz and 2.885 Hz were detected from the dynamic displacement time series of the composite instrument in vertical direction. Also, the modal frequencies of 1.687 Hz and 2.875 Hz were detected from the dynamic displacement time series of the accelerometer in vertical direction. The difference values between the frequencies detected from both the composite instrument and accelerometer are no more than 0.01 Hz, and its difference ratio are less than 0.6%. It is shown that the composite instrument is capable of detection a relatively lower vibration frequencies of the footbridge.

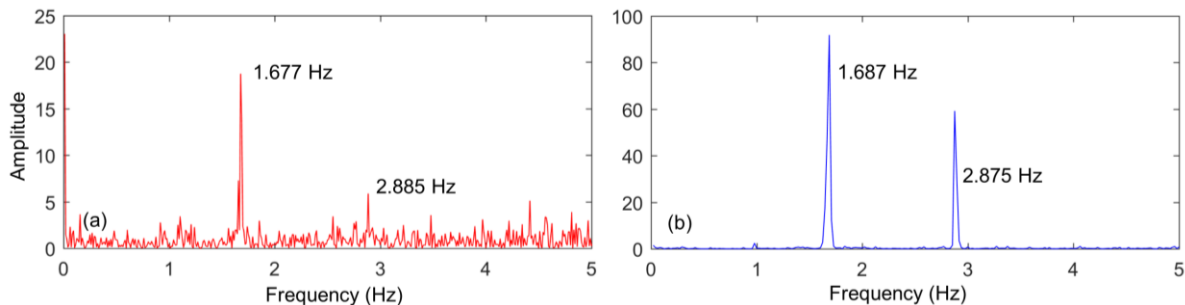


Figure 9. Comparison of FFT-based spectra of two dynamic displacements in vertical direction: (a) Spectrum of the dynamic displacements derived from the composite instrument data, (b) and the one computed from accelerometer data.

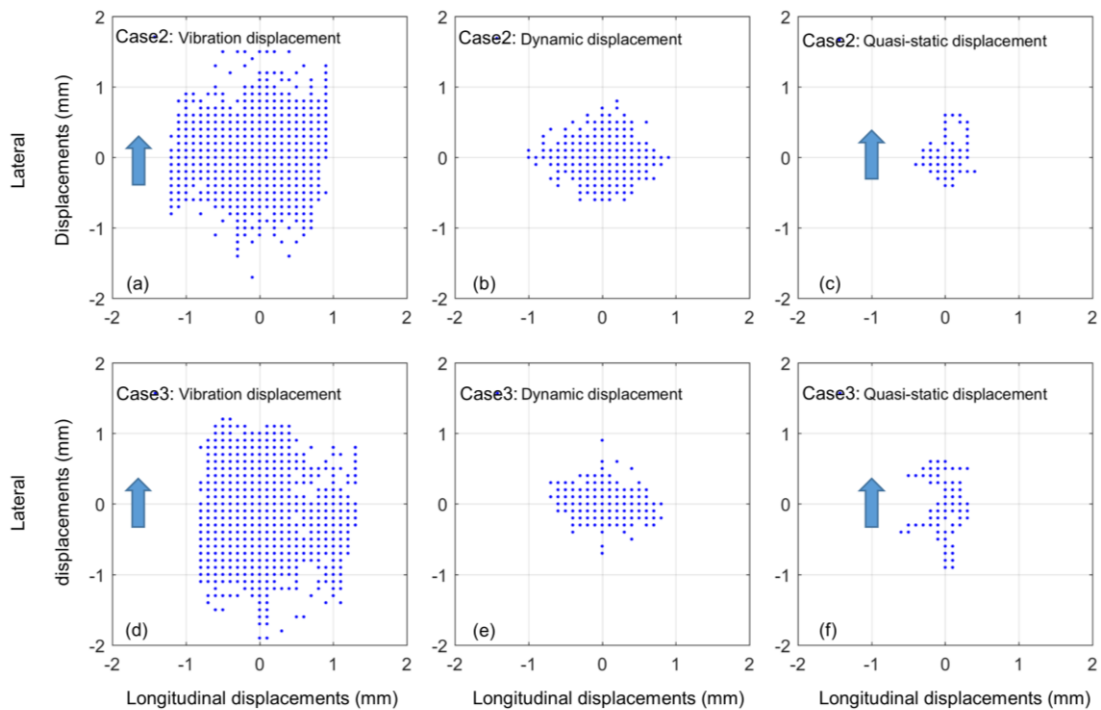


Figure 10. The longitudinal and lateral displacement distribution ranges of the measure-point of the studied footbridge, derived from the composite instrument measurements. The overall vibration displacements (a), dynamic displacements (b) and quasi-static displacements (c) in case 2, and corresponding ones (d, e, f) in case 3. The distribution ranges of both overall vibration displacements and quasi-static displacements in lateral direction are significantly larger than the ones in longitudinal direction because of the wind along the lateral direction (blue arrows).

The distribution ranges of longitudinal and lateral displacements of the measure point of the footbridge are graphically depicted (Figure 10). These displacements were derived from the composite instrument data in two experimental cases 2 and 3. In each case, the distribution range of overall vibration displacements in lateral direction are larger than the one in longitudinal direction. The distribution range of quasi-static displacements show same characteristics. The reason is that the wind along lateral directions cause relatively larger vibrations in lateral direction. It is obvious that a tendency for the increased displacements along the wind direction is evident.

5. Conclusions

A revolutionary surveying system of the composite instrument was proposed to monitor three-dimensional vibration displacements of a footbridge. It is capable of not only detecting quasi-static and dynamic displacements of the footbridge, but also obtaining nanosecond-level time information in each record, which is valuable for multi-sensor data fusion. A CMWT algorithm was developed to understand noise characteristics in the composite instrument measurements in time-frequency domain. Experiments were conducted on the Nottingham Wilford suspension bridge to verify the measurements of vibration displacements of footbridges using the composite instrument. The Chebyshev filter was adopted to separate quasi-static and dynamic displacements from the composite instrument measurements. Both wavelet and FFT algorithms were employed in spectral analyses of displacement time series in time-frequency domain.

Firstly, we verified that the composite instrument possesses a capacity of accurately identifying both quasi-static and dynamic displacements of footbridges with several millimeter amplitudes. Three people jumping-induced dynamic displacements of the footbridge, with displacement peak values from 5.7 to 10 mm, were identified by the composite instrument. Their measurement

accuracies are superior to 1 mm. Quasi-static displacement components of the footbridge can be identified from the composite instrument data with a submillimeter-level accuracy. The corresponding peak differences between two sets of dynamic displacements derived from the composite instrument and accelerometer data, are less than 1.0 mm; their peak difference ratios are no more than 10.0%. In other case study, slightly wind and occasional pedestrian-induced vibration displacements of the footbridge, with peak displacements from 1.3 to 2.5 mm, were accurately identified by the composite instrument. Relatively low vibration frequencies of the footbridge in vertical direction, 1.677 Hz and 2.885 Hz, were identified from the composite instrument measurements.

The second contribution of this study is that the composite instrument measurement noise was characterized in detail by a CMWT algorithm in time-frequency domain. All of the standard deviations of the background noise in each direction are no more than 0.5 mm when the composite instrument is 60 m away from the prism. The main noise energy distributes within a relatively low frequency range of no more than 0.1 Hz.

The composite instrument will be a potential tool for synchronously detecting the quasi-static and dynamic displacements of bridge structures with a satisfied accuracy. The study only concentrates on displacement monitoring of footbridges, but the potential of using the composite instrument to identify the modal frequencies of footbridges would be exploited with its overall performance and data acquisition algorithm improving significantly.

Author Contributions: Conceptualization, J.Y. and X.M.; methodology, J.Y.; software, J.Y.; validation, J.Y., Y.X. and Q.F.; formal analysis, J.Y.; investigation, J.Y., Q.F. and Z.F.; resources, J.Y.; data curation, J.Y.; writing—original draft preparation, J.Y.; writing—review and editing, Z.F.; visualization, J.Y.; supervision, X.M.; project administration, J.Y., X.M.; funding acquisition, J.Y. All authors have read and agreed to the published version of the manuscript.

Funding: This study is supported by the National Key R&D Program of China (No. 2016YFC0800207) and Changsha science and technology project (No. kq1907110).

Acknowledgements: The University of Nottingham is thanked for supplying instruments in field experiments.

Conflicts of Interest: The authors declare no conflicts of interest.

References

1. V.B.G. Esteban, J.R. Gaxiola-Camacho, R. Bennett, G.M. Guzman-Acevedo, I.E. Gaxiola-Camacho, Structural evaluation of dynamic and semi-static displacements of the Juarez Bridge using GPS technology, *Measurement*, 110 (2017) 146-153.
2. F. Moschas, S. Stiros, Dynamic Deflections of a Stiff Footbridge Using 100-Hz GNSS and Accelerometer Data, *J. Surv. Eng.*, 141 (2015) 04015003, 04015001-04015008.
3. T.H. Yi, H.N. Li, M. Gu, Experimental assessment of high-rate GPS receivers for deformation monitoring of bridge, *Measurement*, 46 (2013) 420-432.
4. N. Shen, L. Chen, J. Liu, L. Wang, T. Tao, D. Wu, R. Chen, A Review of Global Navigation Satellite System (GNSS)-based Dynamic Monitoring Technologies for Structural Health Monitoring, *Remote Sensing*, 11 (2019) 1001.
5. J. Yu, X. Meng, B. Yan, B. Xu, Q. Fan, Y. Xie, Global Navigation Satellite System-based positioning technology for structural health monitoring: a review, *Struct. Contr. Health Monit.*, 27 (2020) e2467.
6. J. Yang, J. Li, G. Lin, A simple approach to integration of acceleration data for dynamic soil-structure interaction analysis, *Soil Dyn. Earthquake Eng.*, 26 (2006) 725-734.
7. M. Gindy, R. Vaccaro, H. Nassif, J. Velde, A State-Space Approach for Deriving Bridge Displacement from Acceleration, *Computer-Aided Civil and Infrastructure Engineering*, 23 (2008) 281-290.
8. H. Ingensand, E. Frei, R. Scherrer, Surveying system including an electro-optic total station and a portable receiving apparatus comprising a satellite position-measuring system, in, *Google Patents*, 1993.
9. A. Biasion, A. Cina, M. Pesenti, F. Rinaudo, An integrated GPS and Total Station instrument for cultural heritage surveying: the LEICA SmartStation example, in: *Proceeding Cipa XX international symposium*.

- Torino, 2005.
- 10. Leica, Leica SmartStation-Total Station with integrated GNSS, in, Leica, 2019, pp. <https://leica-geosystems.com/products/total-stations/systems/leica-smartstation>.
 - 11. E. Cosser, G.W. Roberts, X. Meng, A. Dodson, Measuring the dynamic deformation of bridges using a total station, in: S. Stiros, S. Pytharouli (Eds.) 11th FIG Symposium on Deformation Measurements, Geodesy and Geodetic Applications Lab., Patras Univ., Santorini, Greece, 2003, pp. 605–612.
 - 12. H. Erdogan, E. Güllal, Ambient Vibration Measurements of the Bosphorus Suspension Bridge by Total Station and GPS, *Experimental Techniques*, 37 (2013) 16-23.
 - 13. A.P. Psimoulis, S. Stiros, Measuring deflections of a short-span railway bridge using a Robotic total station, *J. Bridge Eng.*, 18 (2013) 182-185.
 - 14. S.C. Stiros, P.A. Psimoulis, Response of a historical short-span railway bridge to passing trains: 3-D deflections and dominant frequencies derived from Robotic Total Station (RTS) measurements, *Eng. Struct.*, 45 (2012) 362-371.
 - 15. F. Moschas, S.C. Stiros, Three-dimensional dynamic deflections and natural frequencies of a stiff footbridge based on measurements of collocated sensors, *Struct. Contr. Health Monit.*, 21 (2014) 23-42.
 - 16. W. Lienhart, M. Ehrhart, M. Grick, High frequent total station measurements for the monitoring of bridge vibrations, *J. Appl. Geod.*, 11 (2017) 1-8.
 - 17. S. Stiros, P. Psimoulis, F. Moschas, V. Saltogianni, E. Tsantopoulos, P. Triantafyllidis, Multi-sensor measurement of dynamic deflections and structural health monitoring of flexible and stiff bridges, *bridge structures*, 15 (2019) 43-51.
 - 18. J. Yu, X. Meng, X. Shao, B. Yan, L. Yang, Identification of Dynamic Displacements and Modal Frequencies of a Medium-Span Suspension Bridge Using Multimode GNSS Processing, *Eng. Struct.*, 81 (2014) 432-443.
 - 19. M. Meo, G. Zumpano, X. Meng, E. Cosser, G. Roberts, A. Dodson, Measurements of dynamic properties of a medium span suspension bridge by using the wavelet transforms, *Mech. Syst. Signal Pr.*, 20 (2006) 1112-1133.
 - 20. W.S. Chan, Y.L. Xu, X.-L. Ding, Y.-L. Xiong, W.-J. Dai, Assessment of dynamic measurement accuracy of GPS in three directions, *J. Surv. Eng.*, 132 (2006) 108-117.
 - 21. J. Yu, P. Zhu, B. Xu, X. Meng, Experimental assessment of high sampling-rate robotic total station for monitoring bridge dynamic responses, *measurement*, 104 (2017) 60-69.
 - 22. B. Cazelles, M. Chavez, G.C.d. Magny, J.-F. Guegan, S. Hales, Time-dependent spectral analysis of epidemiological time-series with wavelets, *Journal of the Royal Society Interface*, 4 (2007) 625-636.
 - 23. J. Yu, B. Yan, X. Meng, X. Shao, H. Ye, Measurement of Bridge Dynamic Responses Using Network-Based Real-Time Kinematic GNSS Technique, *J. Surv. Eng.*, 142 (2016) 04015013.
 - 24. G.W. Roberts, X. Meng, A.H. Dodson, Integrating a Global Positioning System and accelerometers to monitor the deflection of bridges, *J. Surv. Eng.*, 130 (2004) 65-72.
 - 25. J. Wang, X. Meng, C. Qin, J. Yi, Vibration Frequencies Extraction of the Forth Road Bridge Using High Sampling GPS Data, *Shock Vibrat.*, 501 (2016) 191762.
 - 26. X. Meng, A.H. Dodson, G.W. Robert, Detecting bridge dynamics with GPS and triaxial accelerometers, *Eng. Struct.*, 29 (2007) 3178-3184.
 - 27. K.T. Park, S.H. Kim, H.S. Park, K.W. Lee, The determination of bridge displacement using measured acceleration, *Eng. Struct.*, 27 (2005) 371-378.
 - 28. K. Kim, J. Choi, J. Chung, G. Koo, I.-H. Bae, H. Sohn, Structural displacement estimation through multi-rate fusion of accelerometer and RTK-GPS displacement and velocity measurements, *Measurement*, 130 (2018) 223-235.